Published in final edited form as:
J Orthop Res. 2009 December ; 27(12): 1596. doi:10.1002/jor.20938.

Effect of fiber distribution and realignment on the nonlinear and inhomogeneous mechanical properties of human supraspinatus tendon under longitudinal tensile loading

Spencer P. Lake, **Kristin S. Miller**, **Dawn M. Elliott**, and **Louis J. Soslowsky**
McKay Orthopaedic Research Laboratory, Department of Orthopaedic Surgery, University of Pennsylvania, Philadelphia, PA

Abstract

Tendon exhibits nonlinear stress-strain behavior that may be due, in part, to movement of collagen fibers through the extracellular matrix. While a few techniques have been developed to evaluate the fiber architecture of other soft tissues, the organizational behavior of tendon under load has not been determined. The supraspinatus tendon (SST) of the rotator cuff is of particular interest for investigation due to its complex mechanical environment and corresponding inhomogeneity. In addition, SST injury occurs frequently with limited success in treatment strategies, illustrating the need for a better understanding of SST properties. Therefore, the objective of this study was to quantitatively evaluate the inhomogeneous tensile mechanical properties, fiber organization and fiber realignment under load of human SST utilizing a novel polarized light technique. Fiber distributions were found to become more aligned under load, particularly during the low stiffness toe-region, suggesting that fiber realignment may be partly responsible for observed nonlinear behavior. Fiber alignment was found to correlate significantly with mechanical parameters, providing evidence for strong structure-function relationships in tendon. Human SST exhibits complex, inhomogeneous mechanical properties and fiber distributions, perhaps due to its complex loading environment. Surprisingly, histological grade of degeneration did not correlate with mechanical properties.

Keywords

collagen fiber realignment; nonlinear tendon mechanics; structure-function; polarized light; supraspinatus tendon

Introduction

Tendon mechanical behavior is nonlinear and is characterized by an initial low stiffness toe-region, followed by a high stiffness linear-region. This nonlinearity is critical to provide the joint with functional range of motion (low stiffness) as well as stability and force transmission (high stiffness). Restoration of both the nonlinear response and linear stiffness are also crucial for restoring function following repair after injury. The toe-region is commonly associated with the gradual recruitment of crimped collagen fibers and to fiber realignment due to interaction between the fibers and extrafibrillar matrix, while in the linear-region, all collagen fibers are believed to be taut and supporting load (1,2). Despite its crucial contribution to normal function and repair success, tendon nonlinearity has received little attention and the role of fiber realignment in tendon mechanical nonlinearity remains unclear. This is due, in part, to

Corresponding Author: Louis J. Soslowsky, Ph.D., University of Pennsylvania, Department of Orthopaedic Surgery, McKay Orthopaedic Research Laboratory, 424 Stemmler Hall, Philadelphia, PA 19104-6081, ph: 215-898-8653, fx: 215-573-2133, soslowsk@upenn.edu.

the lack of a suitable technique to measure fiber alignment and realignment as a function of stress and strain in tendon.

Several approaches have been used to analyze the fiber architecture of tendon and other fiber-reinforced soft tissues. Previously utilized techniques include optical and scanning electron microscopy (3-5), scattering (x-ray, electron, light) techniques (6-8), optical coherence tomography (2), and an application of fast Fourier transform imaging processing (9). These techniques often require special tissue preparation (such as tissue fixation), complicated equipment set-up, and/or long acquisition times, making them unsuitable for measuring fiber alignment during mechanical testing. Polarized light microscopy has been used successfully to evaluate fiber orientation for several different fiber-reinforced soft tissues including tendon (3,10,11), cartilage (12), ligament (13), muscle (14) and mitral valve (15). Besides its use in microscopy applications, polarized light imaging has been used recently to quantify fiber angles continuously during mechanical testing of heart valve leaflets (16) and ligament (17). While no study has yet quantified fiber realignment during tensile testing in tendon, this relatively simple, non-destructible polarized light imaging technique may provide a suitable approach for examining this behavior.

A particularly interesting tissue for examining nonlinearity and fiber realignment is the human supraspinatus tendon (SST), one of the four rotator cuff tendons in the shoulder. Rotator cuff damage due to degeneration and/or injury is a common cause of significant pain and disability affecting the young and old alike. Different from many tendons, the SST must regularly withstand a complex loading environment consisting of multiaxial tensile forces, compression and shear, which are due to complex neighboring anatomy and the large range of motion of the glenohumeral joint. This complex anatomy is likely responsible for the unique mechanical and organizational properties that have been reported for this tendon. Previous work has described a nonlinear mechanical response of human SST that is consistent with other tendons; however, SST mechanical properties were also found to be highly inhomogeneous (18,19). When the SST was split across the width (anterior to posterior) into three separate test samples, the modulus, failure load and failure stress were found to be highest in the anterior region of the tendon, then decrease posteriorly (18). In addition, two studies that evaluated differences in tensile moduli through the thickness (superior to inferior) indicate small to no difference (18,19). Organizationally, the collagen fiber network of human SST has also been described as being highly inhomogeneous (20,21). Previous studies using histological methods have qualitatively described SST as consisting of up to five distinct layers with varying degrees of collagen fiber alignment through the thickness of the tendon (20). This study also described an apparent splay in fiber orientation near the tendon-bone insertion, suggesting a higher degree of alignment away from the insertion which may have implications for relative mechanical strength along the tendon length. However, the fiber organization of SST has not yet been thoroughly evaluated using a quantitative approach. In addition, the relationship between fiber alignment and mechanical properties has not been evaluated, nor has fiber realignment under load and its potential implications regarding tensile nonlinearity.

Therefore, the objective of this study is to quantitatively evaluate the mechanical properties, fiber organization and fiber realignment under tensile load of human SST, as well as to utilize these data to investigate structure-function relationships of this complex tissue. We hypothesize that (1) mechanical properties will be location-dependent and most stiff in the tendon midsubstance, (2) collagen fiber organization is inhomogeneous and realignment will occur primarily in the toe-region of the mechanical test, and (3) there will be significant correlation between mechanical and organizational properties.

Methods

Sample preparation

Sixteen supraspinatus tendons (SST) were harvested from human cadaveric shoulders (average age 57.4±15.0 years). Donors had no reported history of injury to the shoulder or rotator cuff, and tendons with partial- or full-thickness tears were excluded. All soft tissue was removed from around the tendon, leaving the supraspinatus muscle-tendon unit attached to the humerus. Capsule tissue was then carefully dissected away, the supraspinatus muscle was removed and the tendon was sharply detached from its humeral insertion. Tendon tissue was kept hydrated with phosphate buffered saline (PBS) during dissection, sample preparation and testing. Rectangular full-thickness samples (~20×5mm) were cut parallel (longitudinal) to the tendon long-axis from three distinct tendon locations (Figure 1; anterior, posterior, medial). In addition, a full-thickness tendon piece was cut from the region between the anterior and posterior samples and used for histological processing.

Samples were frozen to a microtome stage (Leica, Wetzlar, Germany) using embedding medium. After leveling off the tendon surface, approximately 200μm of tissue was removed prior to cutting an approximately 400μm-thick tissue slice representing the bursal (superior) tendon surface. The sample was then removed from the microtome, turned over to the opposite side, and refrozen to the stage. Once again the tendon surface was leveled off and approximately 200μm of tissue was removed. An approximately 400μm-thick slice was then cut representing the joint (inferior) surface (order of cutting bursal vs. joint samples was randomized). Thus each shoulder yielded six location-specific test samples (Figure 1): anterior-bursal (AB), anterior-joint (AJ), posterior-bursal (PB), posterior-joint (PJ), medial-bursal (MB), and medial-joint (MJ). Six to eight 0.5mm-diameter brass beads (Small Parts, Miramar, FL) were carefully attached to the tendon surface using a small amount of cyanoacrylate in a grid pattern for strain measurement. The evaluation of this grid of beads, which was placed in the center region of the sample according to St. Venant's principle, provides a more accurate measure of the average strain in this region than other commonly-used techniques (e.g., grip-to-grip strain, measurements between two stain lines). Cross-sectional area was measured using a non-contact, laser device (22) and sample ends were glued between pieces of double-sided sandpaper using cyanoacrylate. Sample width and length were measured using digital calipers. After allowing time for glue to dry, samples were loaded in custom-built aluminum grips prior to testing.

Mechanical testing

Clamped samples were placed in a PBS bath and loaded in a tensile testing machine (Instron, Norwood, MA) integrated with a custom-built polarized light and imaging system to quantify fiber alignment during testing. This system consists of a linear backlight (Dolan-Jenner, Boxborough, MA), two linear polarizing sheets (Edmund Optics, Barrington, NJ) oriented perpendicular to one another on either side of the test sample, a stepper motor (Lin Engineering, Santa Clara, CA) for polarizer rotation, and a high resolution digital camera (Imaging Solutions Group, Fairport, NY) for image acquisition (Figure 2). Prior to testing, the stepper motor encoder count was reset with the polarizer sheets set at a position corresponding to 0° of angular rotation in order to initialize encoder count values. Tendon samples were ramped to failure at a constant strain rate of 0.1%/sec from a slack position to ensure that the toe-region was not inadvertently missed. Based on preliminary studies, a tare stress of 0.0075 MPa was used to establish the zero stress-strain state. Images were acquired every 5 seconds for optical strain analysis. In addition, sets of 15 images were acquired every 10 seconds as the polarizers rotated through a 135° range.

Data analysis

A custom Matlab program (Matlab, Natick, MA) was used to optically track the center point of each of the beads placed on the tendon surface for images throughout the ramp to failure. From these coordinates, two-dimensional Lagrangian strain (E11, E22, and E12) was calculated using tensor algebra to compute the finite deformation gradient, translation vector and subsequent strain values (23). Stress was calculated as force divided by initial cross-sectional area. A bilinear curvefit was applied to the stress-strain data in order to quantify the modulus in the toe- and linear-regions, as well as the stress and strain values corresponding to the transition point of the bilinear fit (Figure 3). Poisson's ratio was calculated as the negative slope of the strain-displacement curve in the transverse direction, divided by the slope of the strain-displacement curve in the loading direction (24).

Fiber alignment was calculated throughout testing from the sets of 15 polarized images. Briefly, images of the tendon surface were divided into rectangular areas (15-wide × 30-long = 450 total areas). Pixel intensities were summed by area, per image and plotted vs. corresponding angle of polarizer rotation. A sine wave was fit to the intensity-angle data using a least-squares curvefit in Matlab. These curvefits were used to determine the angle corresponding to minimum pixel intensity, which represents the average direction of the area's collagen fiber alignment. A limitation of this crossed polarizer method is that fiber angles can only be calculated within a 90° range (±45° to the predominant fiber direction) rather than the full 180° range of possible orientations. To overcome this limitation, fibers were assumed to always rotate towards the loading direction. Angle-time plots were created for each area to evaluate direction of fiber rotation (towards or away from the loading direction). Areas that exhibited angle values that moved away from the loading direction were corrected (±90°) as appropriate. After calculating average angle values for each area, alignment maps and histograms were created by compiling values from all areas (Figure 4). Circular variance (VAR), a measure of the distribution of collagen fiber alignment across the tendon surface, was calculated at zero strain, transition strain (intersection of the toe- and linear-regions) and linear-region strain (2× transition strain). Fiber realignment in the toe region was evaluated by comparing VAR values at the zero and transition strains, while linear-region realignment was evaluated by comparing VAR values at the transition and linear-region strains.

Histology

Full-thickness SST samples (~20×5mm) taken from the region between the anterior and posterior mechanical test samples were used for histological analysis. After dissection, tissue was fixed in 10% neutral buffered formalin for 48 hours. Samples were subjected to a standard processing protocol, embedded in paraffin and sectioned at 7μm. Representative sections from four levels evenly spaced through the thickness were stained with hematoxylin and eosin. Blinded sections were evaluated by two independent graders according to a modified semi-quantitative tendon degeneration grading scheme (25). According to this grading scale, grade 1 corresponds to a strong sense of collagen fiber organization, low cellularity and low vascularity (i.e. healthy tendon). Grade 2 shows regions of strong collagen alignment but lacks consistency and exhibits low to medium levels of cells and vasculature. Grade 3 is demonstrated by general disruption of collagen organization and medium cellularity and vascularity. Finally, grade 4 represents complete disorganization of the collagen fiber network and high levels of cells and vasculature (i.e. highly degenerate tendon). For each section, four images were taken under a microscope (25× magnification) along the length of the sample. A grade was given for each image, at each thickness level, resulting in 16 scores per shoulder per grader. An overall grade was calculated for each shoulder by averaging the combined scores.

Statistical analysis

Shapiro-Wilk tests indicated non-normally distributed data, so non-parametric statistical tests were utilized for all data analysis. For all statistical analyses, significance was set at $p<0.05$, trends at $0.05<p<0.1$ and Bonferroni corrections were made for number of comparisons to remain conservative in our data interpretation. Mechanical parameter values (toe-region modulus, linear-region modulus, Poisson's ratio, transition stress, transition strain) were compared for tendon location (AB, AJ, PB, PJ, MB, MJ) using Kruskal-Wallis tests followed by Mann-Whitney post-hoc tests. Fiber realignment during testing was evaluated within each tendon location using Friedman tests to compare VAR_{zero} to $VAR_{transition}$ (toe-region realignment) and $VAR_{transition}$ to VAR_{linear} (linear-region realignment), followed by Wilcoxon signed-rank post-hoc tests. Spearman rank correlation coefficients were calculated to evaluate correlations between location-specific median modulus values and location-specific median VAR_{zero} values. Finally, the effect of degeneration on mechanical properties was investigated by calculating Spearman rank correlation coefficients between histology grade and each of the mechanical parameters. Due to its non-normality, all data is presented as median and interquartile range.

Results

Moduli values were highly nonlinear (~10× linear/toe region ratio) and highly inhomogeneous (Figure 5). For both toe- and linear-regions, the posterior samples had significantly lower moduli values than both the anterior and medial samples (compared within bursal/joint level), and there was a trend for a higher modulus in medial compared to anterior (MB/AB). There were no differences between bursal and joint moduli values within any of the three locations (A, P, M). This pattern of inhomogeneity was repeated for the transition stress values (Table 1), however only the MJ-PJ comparison was statistically significant. For transition strain values, the posterior bursal values were greater than corresponding anterior and medial samples (Table 1). Median Poisson's ratios for both medial locations were near zero and were significantly less than anterior (Table 1).

Circular variance values (VAR) demonstrate fiber realignment in the toe-region ($VAR_{transition}$-VAR_{zero}) of samples from all tendon locations (Figure 6). In addition, there was significant realignment in the linear-region (VAR_{linear}-$VAR_{transition}$) of the anterior and posterior samples, but not medial samples. The degree of fiber alignment at zero strain was highly dependent on tendon location (Figure 7a). Specifically, the medial samples were more highly aligned than the anterior and posterior samples (compared within bursal/joint level). The anterior samples were also more aligned than the posterior samples within the joint samples (PJ/AJ).

There was a negative correlation between median zero strain variance values and the median linear-region moduli (r_s=-0.83, p=0.058, Figure 7b). There were also significant correlations (not shown) between VAR_{zero} and toe-region modulus (r_s=-1.0, p=0.003), transition strain (r_s=0.89, p=0.033) and transition stress (r_s=-0.94, p=0.017). The correlation for Poisson's ratio was not significant (r_s=0.6, p=0.24).

Average specimen histology grades were distributed over a large range of scores (~1.5 – 3.5) indicating varying levels of degeneration. Due to the semi-quantitative nature of these scores, a rank statistical test (Spearman) was used to evaluate correlation. There were no significant correlations of histology grade with any of the mechanical test parameters (toe- and linear-region modulus, transition stress/strain, and Poisson's ratio), circular variance values or donor age (not shown).

Discussion

This study provides a quantitative description of the collagen fiber organization of supraspinatus tendon samples and examines how that fiber distribution realigns under uniaxial tension. Fiber distributions were seen to become more highly aligned when samples were loaded, consistent with work in other soft biological tissues (9,16). We hypothesized that fiber realignment would occur primarily in the toe-region of the stress-strain response, which would suggest that nonlinear tendon mechanics may be due, at least in part, to movement of the fibers through the extrafibrillar matrix. While there was significant realignment in the toe-region for all tendon locations, there was also significant realignment during the linear-region in four of the six specimen groups. The medial samples (MB, MJ) were seen to only experience fiber realignment during the toe-region, perhaps due to the much higher degree of initial fiber alignment. These results indicate that fiber realignment may contribute to mechanical nonlinearity, especially in highly aligned tissues. However in the anterior and posterior locations evaluated in this study, which are much less aligned than the medial samples, realignment occurred throughout the loading protocol indicating that other factors must also be responsible for the observed nonlinear stress-strain response. One likely contributor is collagen uncrimping with load. Collagen fibril crimp was not evaluated in the current study because of the small scale at which it occurs relative to the fiber-level measurements examined here. However, several studies have demonstrated that the crimping pattern observed in slack collagen fibrils disappears when relatively small magnitude levels of strain are applied to tendon/ligament samples, suggesting that the toe-region stress-strain response is due to the gradual recruitment of fibril straightening (2,4-6). It is likely that tendon nonlinearity is due to several contributing/interacting factors, of which both fiber realignment and fibril uncrimping play a role.

In agreement with our hypothesis, there were strong correlations between the initial fiber alignment (at zero strain) and mechanical properties. Toe-region modulus, linear-region modulus and transition stress all exhibited significant negative correlations with VAR_{zero} values. Thus, the degree to which collagen fibers are initially aligned predicts the subsequent mechanical response, with higher initial alignment (small VAR values) corresponding to higher (stiffer) mechanical properties. Transition strain, on the other hand, had a significant positive correlation with zero strain variance values. In other words, samples with less aligned initial fiber distributions were strained to a larger degree (a longer toe-region) before transitioning to the linear-region. For example, the median transition value for samples from the highly-aligned medial locations was 2.6% strain compared to a median value of 6.4% transition strain for the less-aligned posterior samples. These two groups also experienced very different amounts of fiber realignment during the toe-region. VAR values decreased by an order of magnitude greater for the posterior samples than the medial samples during the toe-region (median $\Delta VAR = 0.030$ and 0.001, respectively). Therefore, not only does the initial collagen fiber alignment correlate with mechanical behavior, but subsequent realignment data is strongly related as well. Taken together, these correlations demonstrate strong structure-function relationships in SST tendon.

This study reports the mechanical properties of samples from six specific locations of the human SST. In agreement with our hypothesis, the properties were inhomogeneous and most stiff in the medial samples. While this is the first study to report the mechanical properties of the medial SST, the pattern of linear-region moduli inhomogeneity for the anterior and posterior samples agrees with previous work. Specifically, moduli values decreased in an anterior-posterior direction and there were no consistent differences between bursal-joint samples (18,19). In our study, the ratio of anterior/posterior linear-region moduli values was approximately 3.2 compared to an approximate ratio of 2.6 in the study by Itoi et al., with a approximate range of moduli values of ~10-140 MPa and ~45-170 MPa, respectively for the

two studies (18). Given the differences in testing protocols, this represents strong consistency between data from these two studies.

In addition to inhomogeneous mechanical parameters, this study also presents quantitative fiber alignment data demonstrating organizational inhomogeneity for human SST. The fiber distributions and tensile properties of SST may be due to the complex loading environment of the rotator cuff. The anterior and posterior locations were less aligned and had smaller moduli values than the medial location. This may be due to the complex multiaxial loads that these locations experience, such as off-axis loads near the tendon-bone insertion or due to acromial impingement. The medial samples, on the other hand, are located away from both the insertion site and the acromion and exhibit higher moduli and high levels of fiber alignment consistent with more typical tendons. Finally, it is possible that the less stiff posterior tissue may be responsible for tear initiation and propagation of supraspinatus tears in the posterior direction observed clinically.

Surprisingly, there were no significant correlations between mechanical parameters and histological grade. Sano et al (26) reported a significant negative correlation between ultimate tensile stress and degeneration score when testing strips of SST still attached to the humerus. However, this previous study only assessed degeneration at the insertion, did not exclude partial SST tears prior to testing, and did not evaluate any other mechanical parameters (such as modulus). It is likely that shoulders with partial- or full-thickness tears have more overall degeneration than non-torn shoulders; however our study excluded shoulders with tendon tears. While our histology scores did span a relatively large range of our grading scale, it is possible that they remain in the lower range of all possible levels of degeneration due to the exclusion of torn tendons. Alternatively, moduli in human SST could truly be independent of degeneration, similar to human annulus fibrosus tissue (27,28). Due to a lack of distinction between normal (“healthy”) and degenerate samples, all data was grouped together for this study.

This study is not without limitations. First, the crossed polarizer method developed and utilized in this study can only measure fibers ±45° of the tendon long-axis (90° total range), instead of the full ±90° that contains all possible fiber orientations (180° total range). While other methods could have been used to quantify fiber angle, we selected the cross-polarizer method as the simplest for setup and analysis that would provide the data needed. This required us to make angle value corrections based on the requirement that fibers must reorient towards the direction of loading. Second, there is a certain degree of anatomical variability in human cadaver tissue making it difficult to harvest tissue samples from identical locations across different tendon specimens. In order to maximize the repeatability of harvest location (across length/width and through thickness), a single individual prepared every sample according to a consistent protocol. Given the significant differences observed in this data set, we conclude that this limitation had a negligible effect.

In conclusion, this study provided insight into the current understanding of tendon fiber organization, fiber realignment under load and how these organizational characteristics correspond to mechanical nonlinearity. This study has also provided valuable data regarding the specific mechanical and organizational properties of human SST. This data is necessary if clinicians are to properly understand, predict, prevent, and treat supraspinatus degeneration and injury. This study has greatly enhanced the current understanding of the complex properties of this tissue and demonstrated the strong correlation between mechanical/organizational properties. When planning treatment or replacement strategies for SST injury and disease, surgeons must appreciate this complexity and the nature of SST structure-function relationships, which indicate the importance of maintaining or restoring the native structural organization in order to preserve mechanical integrity. In addition, the organizational and

mechanical data presented here can provide vital guidelines for developing tissue-engineered tendon replacements. Future work will utilize multiaxial loading and mathematical models to further investigate properties and structure-function relationships of tendon.

Acknowledgments

This study was supported by a grant from the NIH/NIAMS (AR055598) and the NIH/NIAMS supported Penn Center for Musculoskeletal Disorders (AR050950). We also thank Spencer Szczesny and Bob Caron for assistance.

References

1. Woo, SL.; An, KN.; Frank, CB., et al. Anatomy, biology, and biomechanics of tendon and ligament. In: Buckwalter, JA.; Einhorn, TA.; Simon, SR., editors. Orthopaedic basic science: Biology and biomechanics of the musculoskeletal system. Second. American Academy of Orthopaedic Surgeons; 2000. p. 581-616.
2. Hansen KA, Weiss JA, Barton JK. Recruitment of tendon crimp with applied tensile strain. J Biomech Eng 2002;124:72–77. [PubMed: 11871607]
3. Whittaker P, Canham PB. Demonstration of quantitative fabric analysis of tendon collagen using two-dimensional polarized light microscopy. Matrix 1991;11:56–62. [PubMed: 2027329]
4. Boorman RS, Norman T, Matsen FA 3rd, Clark JM. Using a freeze substitution fixation technique and histological crimp analysis for characterizing regions of strain in ligaments loaded in situ. J Orthop Res 2006;24:793–799. [PubMed: 16514649]
5. Hurschler C, Provenzano PP, Vanderby R Jr. Scanning electron microscopic characterization of healing and normal rat ligament microstructure under slack and loaded conditions. Connect Tissue Res 2003;44:59–68. [PubMed: 12745672]
6. Morgan M, Kostyuk O, Brown RA, Mudera V. In situ monitoring of tendon structural changes by elastic scattering spectroscopy: Correlation with changes in collagen fibril diameter and crimp. Tissue Eng 2006;12:1821–1831. [PubMed: 16889512]
7. Kirby MC, Aspden RM, Hukins DWL. Determination of the orientation distribution function for collagen fibrils in a connective tissue site from a high-angle x-ray diffraction pattern. J Appl Cryst 1988;21:929–934.
8. Sacks MS, Smith DB, Hiester ED. A small angle light scattering device for planar connective tissue microstructural analysis. Ann Biomed Eng 1997;25:678–689. [PubMed: 9236980]
9. Guerin HA, Elliott DM. Degeneration affects the fiber reorientation of human annulus fibrosus under tensile load. J Biomech 2006;39:1410–1418. [PubMed: 15950233]
10. Dickey JP, Hewlett BR, Dumas GA, Bednar DA. Measuring collagen fiber orientation: A two-dimensional quantitative macroscopic technique. J Biomech Eng 1998;120:537–540. [PubMed: 10412427]
11. Thomopoulos S, Williams GR, Gimbel JA, et al. Variation of biomechanical, structural, and compositional properties along the tendon to bone insertion site. Journal of Orthopaedic Research 2003;21:413–419. [PubMed: 12706013]
12. LeRoux MA, Arokoski J, Vail TP, et al. Simultaneous changes in the mechanical properties, quantitative collagen organization, and proteoglycan concentration of articular cartilage following canine meniscectomy. J Orthop Res 2000;18:383–392. [PubMed: 10937624]
13. Staszyk C, Wulff W, Jacob HG, Gasse H. Collagen fiber architecture of the periodontal ligament in equine cheek teeth. J Vet Dent 2006;23:143–147. [PubMed: 17022193]
14. Toylor DL. Quantitative studies on the polarization optical properties of striated muscle. I. Birefringence changes of rabbit psoas muscle in the transition from rigor to relaxed state. J Cell Biol 1976;68:497–511. [PubMed: 16016]
15. Kunzelman KS, Cochran RP. Stress/strain characteristics of porcine mitral valve tissue: Parallel versus perpendicular collagen orientation. J Card Surg 1992;7:71–78. [PubMed: 1554980]
16. Tower TT, Neidert MR, Tranquillo RT. Fiber alignment imaging during mechanical testing of soft tissues. Ann Biomed Eng 2002;30:1221–1233. [PubMed: 12540198]

17. Quinn KP, Winkelstein BA. Altered collagen fiber kinematics define the onset of localized ligament damage during loading. J Appl Physiol 2008;105:1881–1888. [PubMed: 18845780]
18. Itoi E, Berglund LJ, Grabowski JJ, et al. Tensile properties of the supraspinatus tendon. J Orthop Res 1995;13:578–584. [PubMed: 7674074]
19. Nakajima T, Rokuuma N, Hamada K, et al. Histologic and biomechanical characteristics of the supraspinatus tendon: Reference to rotator cuff tearing. Journal of Shoulder & Elbow Surgery 1994;3:79–87.
20. Clark JM, Harryman DT 2nd. Tendons, ligaments, and capsule of the rotator cuff. Gross and microscopic anatomy. J Bone Joint Surg Am 1992;74:713–725. [PubMed: 1624486]
21. Gohlke F, Essigkrug B, Schmitz F. The pattern of the collagen fiber bundles of the capsule of the glenohumeral joint. Journal of Shoulder & Elbow Surgery 1994;3:111–128.
22. Favata, M. PhD. University of Pennsylvania; Philadelphia: 2006. Scarless healing in the fetus: Implications and strategies for postnatal tendon repair.
23. Thomopoulos S, Fomovsky GM, Chandran PL, Holmes JW. Collagen fiber alignment does not explain mechanical anisotropy in fibroblast populated collagen gels. J Biomech Eng 2007;129:642–650. [PubMed: 17887889]
24. Lynch HA, Johannessen W, Wu JP, et al. Effect of fiber orientation and strain rate on the nonlinear uniaxial tensile material properties of tendon. J Biomech Eng 2003;125:726–731. [PubMed: 14618932]
25. Riley GP, Goddard MJ, Hazleman BL. Histopathological assessment and pathological significance of matrix degeneration in supraspinatus tendons. Rheumatology (Oxford) 2001;40:229–230. [PubMed: 11257166]
26. Sano H, Ishii H, Yeadon A, et al. Degeneration at the insertion weakens the tensile strength of the supraspinatus tendon: A comparative mechanical and histologic study of the bone-tendon complex. J Orthop Res 1997;15:719–726. [PubMed: 9420602]
27. Acaroglu ER, Iatridis JC, Setton LA, et al. Degeneration and aging affect the tensile behavior of human lumbar anulus fibrosus. Spine 1995;20:2690–2701. [PubMed: 8747247]
28. O'Connell GD, Guerin HL, Elliott DM. Theoretical and uniaxial experimental evaluation of human annulus fibrosus degeneration. J Biomech Eng. In press.

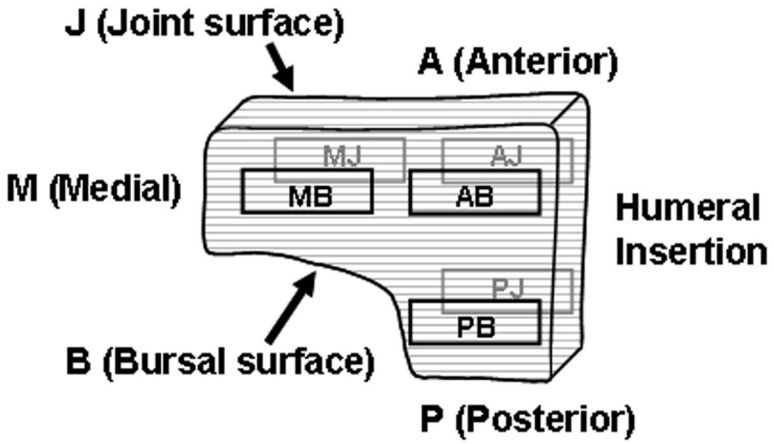

Figure 1.
Harvest location of six human supraspinatus tendon samples (schematic represents a tendon taken from a right shoulder)

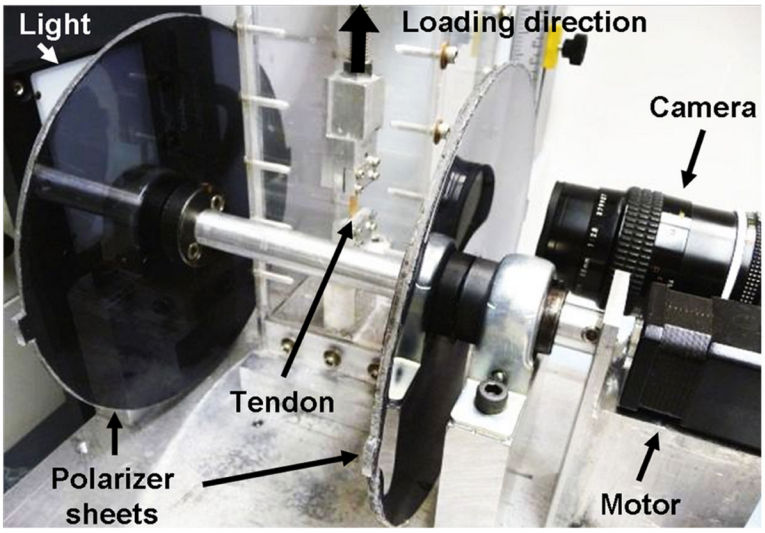

Figure 2.
Angled side-view of tendon tensile testing setup showing polarized light and imaging system: light source, rotating cross-polarized sheets, stepper motor and camera.

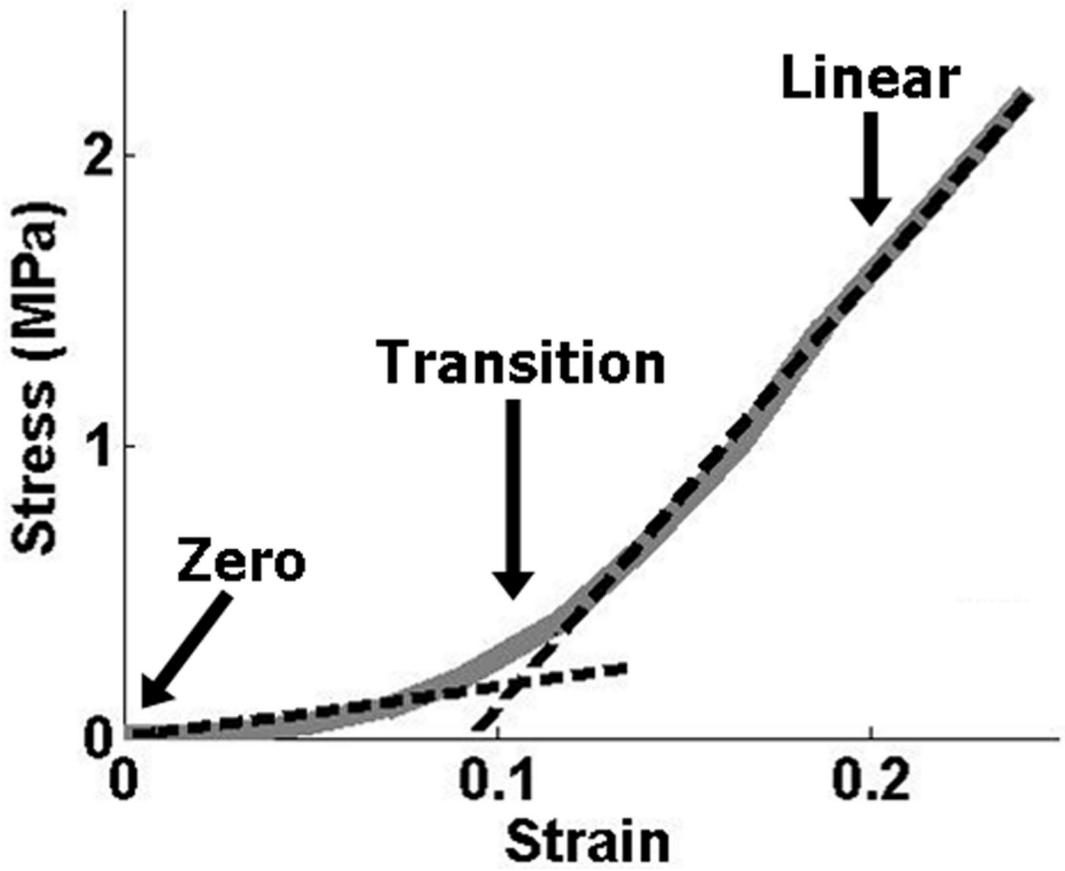

Figure 3.
Example bilinear curvefit of stress-strain tensile data; arrows indicate the zero, transition and linear strain values

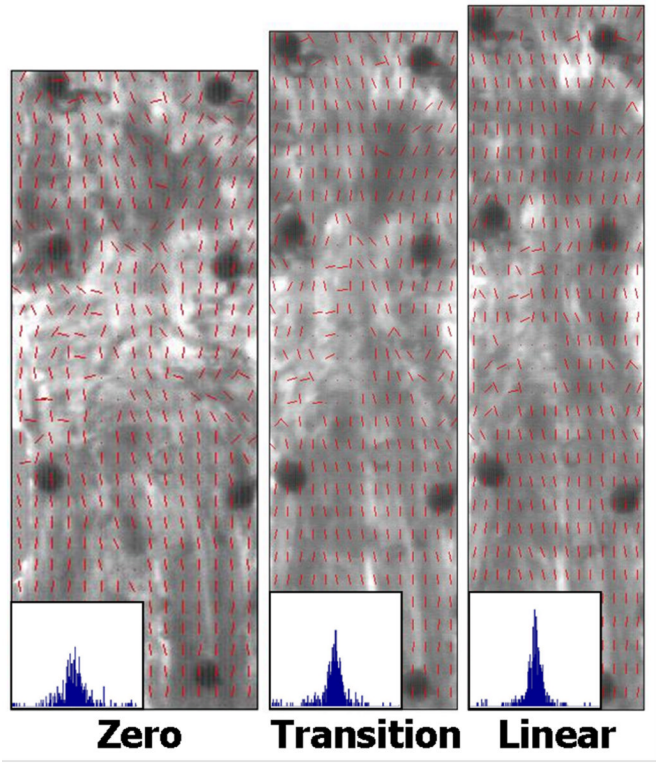

Figure 4.
Sample alignment maps and histograms at zero, transition and linear strain levels demonstrate increasing fiber alignment with increased strain (VAR values = 0.12, 0.09, and 0.06, respectively)

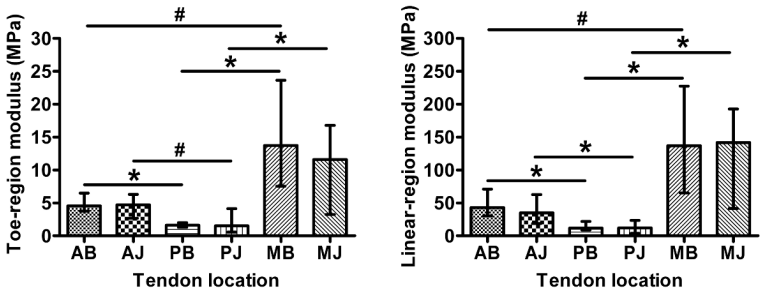

Figure 5.
Modulus in the toe- (left) and linear-region (right) depict inhomogeneous and nonlinear (note scale of y-axes) tensile properties of supraspinatus tendon (median and interquartile range; *=significant, #=trend)

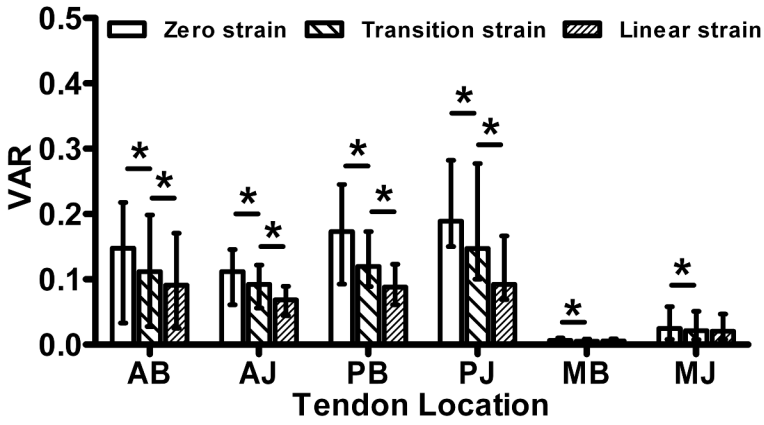

Figure 6.

Circular variance values (VAR) show inhomogeneous fiber distributions, increasing alignment in the toe-region (zero to transition strain) of all tendon locations and in the linear-region (transition to linear strain) of anterior (AB, AJ) and posterior (PB, PJ) samples (median and interquartile range; *=significant, #=trend)

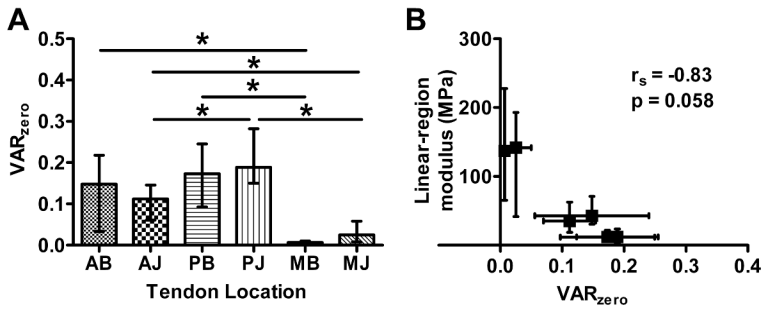

Figure 7.

(A) VAR values at zero strain demonstrate organizational inhomogeneity; (B) median VAR values correlate significantly with mechanical parameters such as linear-region modulus (r_S=Spearman rank correlation coefficient); (both plots depict median and interquartile range;*=significant)

Table 1

Median and interquartile ranges for transition strain, transition stress and Poisson's ratio for human supraspinatus tendon (matching letters indicate statistically significant differences, $p<0.05$)

	Transition strain				Transition stress (MPa)				Poisson's ratio			
	25%	Median	75%		25%	Median	75%		25%	Median	75%	
AB	0.03	**0.04**	0.05	**a**	0.11	**0.19**	0.31		0.84	**1.27**	1.61	**d**
AJ	0.03	**0.04**	0.05		0.09	**0.18**	0.31		1.22	**1.79**	2.07	**e**
PB	0.04	**0.06**	0.12	**a,b**	0.07	**0.12**	0.24		0.69	**0.97**	1.36	
PJ	0.04	**0.06**	0.09		0.04	**0.08**	0.19	**c**	0.72	**1.28**	1.72	
MB	0.02	**0.03**	0.04	**b**	0.12	**0.37**	0.74		-0.49	**0.25**	1.01	**d**
MJ	0.02	**0.03**	0.04		0.14	**0.29**	0.49	**c**	-0.11	**0.96**	1.17	**e**